THE ASTROPHYSICAL JOURNAL, 364:173–177, 1990 November 20

OBSERVATIONS OF THE DENSE GAS IN THE IRAS 16293−2422 OUTFLOW SYSTEM

CHRISTOPHER K. WALKER
California Institute of Technology

JOHN E. CARLSTROM[1] AND JOHN H. BIEGING
University of California at Berkeley

AND

CHARLES J. LADA AND ERICK T. YOUNG
Steward Observatory

Received 1990 January 8; accepted 1990 May 11

ABSTRACT

We present millimeter-wave interferometric and single-dish observations of *IRAS* 16293−2422 in the CS $J = 2 \rightarrow 1$ line. The images reveal clumpy, shell-like structures which appear to be limb-brightened emission from dense gas at the perimeter of the molecular outflow observed in CO. These structures may be ambient cloud material swept up by a stellar wind into dense shells. At all velocities where CS is detected, features related to the outflow are observed. Most of the mass of the outflow system is contained in low-velocity shells.

Subject headings: interstellar: molecules — nebulae: internal motions

I. INTRODUCTION

The infrared source *IRAS* 16293−2422 (hereafter 1629a) is enshrouded in a cold, dense molecular cloud core located in the eastern streamer region of the Rho Ophiuchi molecular cloud complex. An unusual molecular outflow (Walker *et al.* 1985; Walker *et al.* 1986; Fukui *et al.* 1986; Wootten and Loren 1987; Walker *et al.* 1988), water maser emission (Wilking and Claussen 1987), and two $\lambda 2$ cm continuum sources (Wootten 1989) are observed toward 1629a. These observations indicate that 1629a contains one or more young stellar objects in the last stages of formation.

The molecular outflow associated with 1629a is unusual because four separate lobes of high-velocity material are observed. A typical outflow source has a bipolar morphology: the line-of-sight velocity of the emission in one lobe is blue-shifted with respect to the central source while the emission in the other lobe is redshifted. Walker *et al.* (1985) found the 1629a system to be quadrupolar when observed with a spatial resolution of 30″ in the CO $J = 2 \rightarrow 1$ transition. They suggested that two separate bipolar outflows are present. A redshifted lobe to the northeast of the infrared source and a blueshifted lobe to the southwest form one system, and a redshifted lobe to the west and a blueshifted lobe to the east form the other system.

Walker *et al.* (1988) noted that (1) the molecular emission from the outflow is clumpy, and (2) there is a tendency for higher velocity clumps to be located at greater distances from the embedded IR source. They suggested an outflow model in which protostellar winds have swept the ambient cloud material into dense, low-velocity shells. The higher velocity clumps move through the low-density cavities left behind. This outflow morphology has been suggested by many authors (Snell, Loren, and Plambeck 1980; Bally and Lada 1983; Snell *et al.* 1984; Lada 1985).

In this paper we present the results of a combined single-dish and interferometric study of dense molecular gas toward the 1629a outflow system. The properties of the dense gas associated with the central core will be discussed in a future paper. The single-dish data are used to investigate the properties of the dense gas and map the large scale structure of the outflow. The interferometric data provide sufficient resolution to image the outflow lobes and search for shell-like structures.

II. OBSERVATIONS

Single-dish observations of $C^{32}S$ and $C^{34}S$ $J = 2 \rightarrow 1$ emission were made with the NRAO 12 m telescope[2] in 1986 October, 1987 February, 1987 July, and 1989 June. The $C^{32}S$ $J = 2 \rightarrow 1$ (97.981 GHz) observations were made toward 70 positions. The central 25 positions around 1629a were taken at half beamwidth (30″) spacings so that the spectra could be combined with the interferometer data. The rest of the observations were made at 40″ spacings. The $C^{34}S$ $J = 2 \rightarrow 1$ (96.413 GHz) observations were made toward 14 positions. A long integration $C^{34}S$ observation was made toward the central IR source. The spectra were obtained simultaneously with 100 kHz and 30 kHz wide channels to obtain velocity resolutions of 0.3 km s^{-1} and 0.09 km s^{-1}, respectively.

Interferometric observations of $C^{32}S$ $J = 2 \rightarrow 1$ emission were made with the Hat Creek millimeter array[3] between 1988 March and 1988 November. A total of 18 configurations of the three 6 m antennas were used to obtain data with 35 different baselines with projected lengths from 2 kλ to 100 kλ. The single-dish and interferometer data sample well all angular scales from 2″ to 120″ over a 120″ field centered on 1629a. The spectral resolution of the Hat Creek CS observations is 0.39 kHz or 0.12 km s^{-1}. Spectral channel maps of the single-dish (12 m) data were Fourier transformed to the visibility plane, combined with the interferometer data and transformed back into maps. The visibility data were suitably weighted to yield a synthesized beam with FWHM of 11″, a compromise between

[1] Currently at the California Institute of Technology.

[2] The National Radio Astronomy Observatory is operated by Associated Universities Inc., under contract to the National Science Foundation.

[3] Operated by the University of California at Berkeley, the University of Illinois, and the University of Maryland, with support from the National Science Foundation.

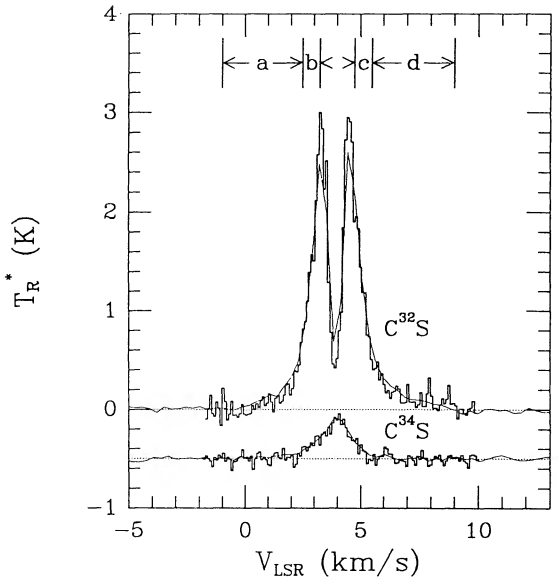

Fig. 1.—$C^{32}S$ and $C^{34}S$ $J = 2 \rightarrow 1$ spectra observed toward *IRAS* 1629a. The $C^{34}S$ spectrum is offset 0.5 K from the $C^{32}S$ spectrum. The 30 kHz specta are shown as histograms. The 100 kHz spectra are shown by smooth lines. The velocity intervals marked *a*, *b*, *c*, and *d* correspond to the V_{LSR} velocity ranges −1–2.5, 2.5–3.125, 4.875–5.5, and 5.5–9 km s^{-1}, respectively.

high-resolution and brightness sensitivity. The maps were cleaned using an 11″ Gaussian restoring beam.

III. RESULTS AND ANALYSIS

a) Single-Dish Data: Large-Scale Structure

The single dish $C^{32}S$ $J = 2 \rightarrow 1$ spectra are, in general, double-peaked and asymmetric, showing a deep, narrow self-absorption feature near the rest velocity of the cloud (4 km s^{-1}). In contrast, the $C^{34}S$ $J = 2 \rightarrow 1$ are single-peaked; they do not show a self-absorption. Spectra of the two isotopes are plotted in Figure 1. The $C^{32}S$ line profile appears to consist of low- and high-velocity components on both the blue- and redshifted sides. These velocity components are indicated in Figure 1.

In Figure 2 we show contour maps made from the single-dish data of the blue- and redshifted $C^{32}S$ emission integrated over both the low- and high-velocity ranges. The redshifted CS emission is strongest in the vicinity of the IR source (marked by the star) with an elongation to the east. The blueshifted emission is strongest to the east and south. Comparison of Figure 2 with the CO $J = 2 \rightarrow 1$ maps in Walker *et al.* (1988) reveals that CS and CO emission show the same general morphology, although the resolution of the CO maps at 30″ is twice as good as the CS single-dish maps (see also Wootten and Loren 1987 and Fukui *et al.* 1986).

We also made individual maps of the low and high velocity components. The low-velocity emission is brightest at the position of the IR source. The maxima in the high-velocity emission are displaced relative to the IR source. The displacement of the higher velocity gas was also seen in CO by Walker *et al.* (1988).

Figure 2 reveals secondary peaks in both the red- and blueshifted CS emission ∼170″ east of the IR source. Emission at all velocities outside the self-absorption range is detected toward this eastern region. One may interpret these secondary emission features as evidence for a separate outflow with an origin ∼170″ east of 1629a. However, there is no known infrared source in the area. Observations of NH_3 DCO^+ by Wootten and Loren (1987) revealed a cold dense concentration of quiescent gas located ∼110″ east of 1629a, a position which very nearly coincides with the saddle point in the dashed (i.e., blueshifted) contours in Figure 2. Wootten and Loren suggest that the increase in the DCO^+ linewidth toward 1629a implies an interaction between the cold quiescent gas and the 1629a outflow. In this context, the secondary CS peaks seen in Figure 2 ∼170″ east of 1629a may trace the eastern blue lobe of the 1629a outflow after it has been deflected by the quiescent clump. The clump is blueshifted with respect to the surrounding cloud and may have been accelerated by the action of the 1629a outflow. The presence of both red- and blueshifted emission at the same position on the sky suggests that the flow has been deflected to lie nearly in the plane of the sky. Similar outflow morphologies have been observed toward B335 and RNO 43 by Cabrit, Goldsmith, and Snell (1988).

b) Interferometer Data: Evidence for Shell Structures

Maps made with the combined interferometer and single dish data are presented in Figures 3 and 4.

Images of the redshifted high- and low-velocity emission are

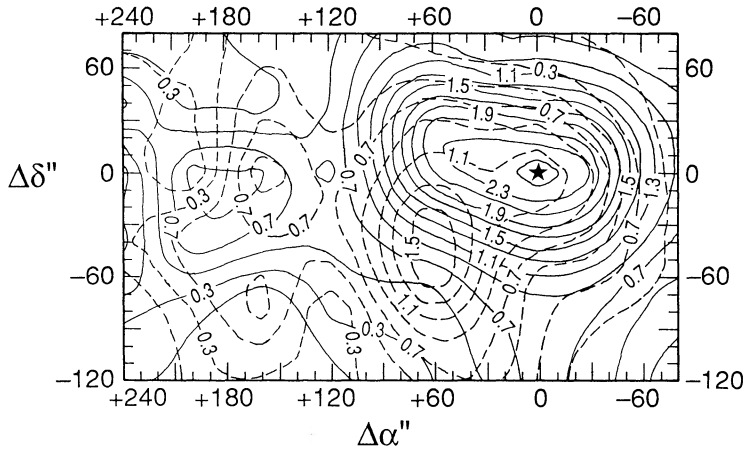

FIG. 2.—Integrated intensity maps of the red and blue shifted CS emission observed toward *IRAS* 1629a with the NRAO 12 m telescope. Dashed and solid lines trace the emission over the V_{LSR} velocity ranges 0.33–3.26 and 4.45–9.0 km s^{-1}, respectively. Contour units are in K km s^{-1}.

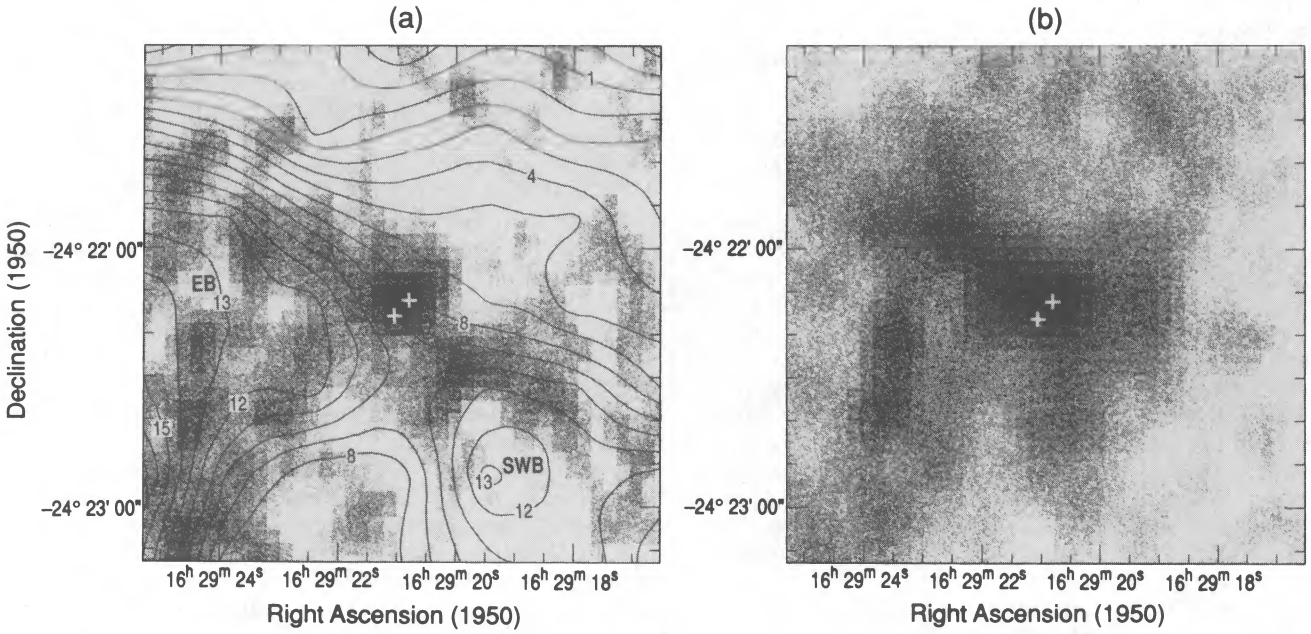

FIG. 3.—Image of the red shifted CS emission in the vicinity of *IRAS* 1629a. (*a*) CS (*linear gray scale*) and ^{12}CO (*contours*) emission over the V_{LSR} velocity range 5.5–9.0 km s^{-1} (interval *d* in Fig. 1). The rms noise level is 0.48 K. The two red shifted outflow lobes are labeled northeastern (NER) and western red (WR). White and black correspond to 0 and 2.28 K, respectively. (*b*) CS emission over the V_{LSR} velocity interval 4.875–5.5 km s^{-1} (interval *c* in Fig. 1). The rms noise level is 1.1 K. White crosses indicate the positions of the two radio continuum sources. White and black correspond to 0 and 10.4 K, respectively.

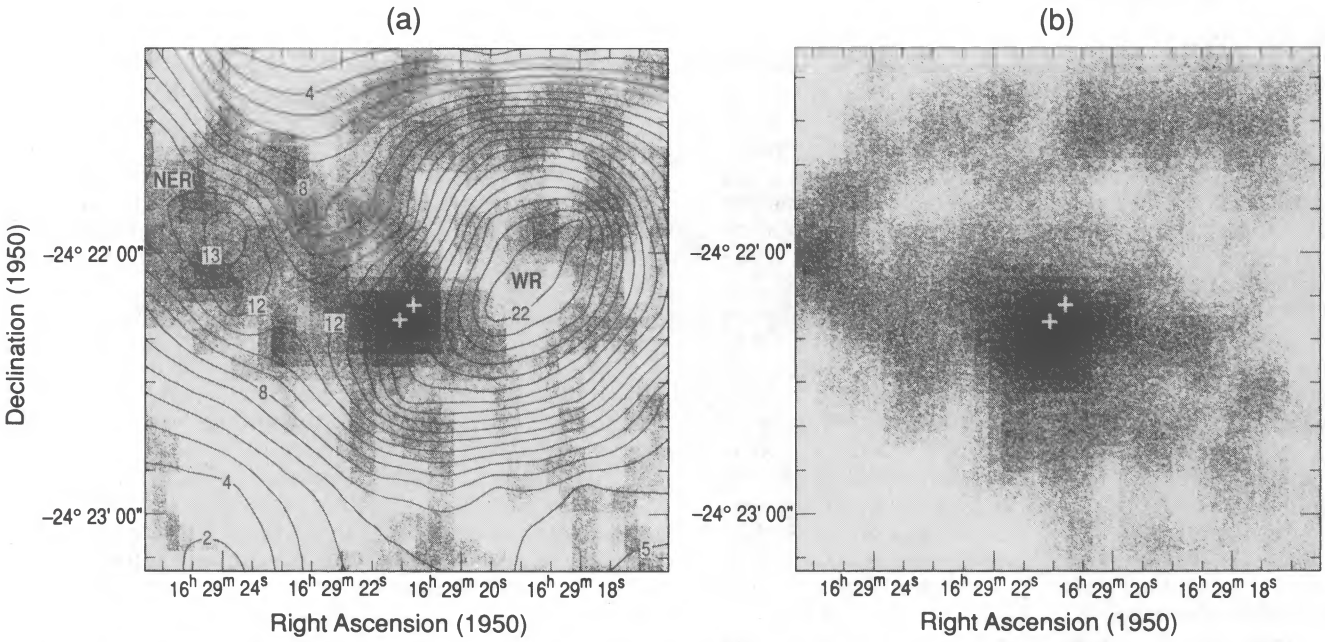

FIG. 4.—Image of the blue shifted CS emission in the vicinity of *IRAS* 1629a. (*a*) CS (*linear gray scale*) and ^{12}CO (*contours*) emission over the V_{LSR} velocity range −1–2.5 km s^{-1} (interval *a* in Fig. 1). The rms noise level is 0.48 K. The two blue shifted lobes are labeled eastern blue (EB) and southwestern blue (SWB). White and black correspond to 0 and 2.22 K, respectively. (*b*) CS emission over the V_{LSR} velocity range 2.5–3.125 km s^{-1} (interval *b* in Fig. 1). The rms noise level is 1.1 K. White crosses indicate the positions of the two radio continuum sources. White and black correspond to 0 and 11.7 K, respectively.

shown in Figure 3. The images of the blueshifted high- and low-velocity emission are shown in Figure 4. Overlaid on the high-velocity images are contours of the CO $J = 2 \rightarrow 1$ emission integrated over the same velocity intervals, from Walker *et al.* (1988). The positions of the two radio sources found by Wootten (1989) are indicated with white crosses.

The images show these features:

1. The high velocity CS brightness distribution is similar to what is seen in the CO $J = 2 \rightarrow 1$ transition at 30″ resolution and suggests the presence of four outflow lobes.

2. The peak in the CS emission reveals the presence of a core structure with a half-power size of $\sim 14''$. The core probably plays an essential role in collimating the flow. This suggests that the outflow is collimated within 7″ of the *IRAS* source.

3. The dense gas, as traced by the CS emission, is very clumpy and occurs within the boundaries of the CO lobes.

4. In the western red (WR) lobe (see Fig. 3[*a*]) it appears that gas has been swept up into a dense ring or shell, with little or no emission from dense gas within. The appearance of the CS emission associated with the northeast red (NER), southwestern blue (SWB), and eastern blue (EB) lobes (see Figs. 3[*a*] and 4[*a*]) also suggest the presence of shell-like structures. In general, the brightest CS emission occurs along the perimeter of the corresponding CO lobes.

5. Many of the features apparent in the images of the high-velocity emission are also present in the low-velocity images. This resemblance provides evidence that the outflow has a strong influence on line formation, even at the lowest observed velocities. Figures 3 and 4 show that the brightest CS emission at all velocities is strongly concentrated toward the IR source.

A map was also made at the velocity of the self-absorption dip seen in the line profiles. It shows the absorbing layer is more or less uniformly distributed over the region.

c) The CS *to* ^{13}CO *Abundance Ratio*

Hartquist, Oppenheimer, and Dalgarno (1980) suggest that the relative abundance of CS may be enhanced in shocked regions. Their results indicate that shocks are capable of driving endothermic chemical reactions causing an overabundance of sulfur-bearing molecules such as CS. Thronson and Lada (1984) and Takano (1986) found that the fractional abundance of CS is one to two orders of magnitude higher in outflow sources (which must be shocked regions) than in quiescent clouds.

The column density of CS toward 1629a can be compared to that of ^{13}CO, which is not expected to be affected by shocks. The ^{13}CO column density integrated over velocities corresponding to the high-velocity (5.36–11.48 km s^{-1} V_{LSR}) CS emission is provided by Walker *et al.* (1988). The CS column density over this interval cannot be easily determined using an isotopic analysis, because C^{34}S emission was not detected at these velocities. However, a stringent lower limit to the CS column density can be calculated under the assumption that the CS emission is optically thin. The column density is then only a function of the integrated intensity and excitation temperature (T_{ex}). From the observed peak brightness temperature in the interferometer maps of the highest velocity gas (see Fig. 1), we estimate that $T_{ex} > 6$ K. Adopting this value and using the expression for CS column density given in Thronson and Lada (1984), we estimate the CS column density to be $\approx 3 \times 10^{12}$ cm^{-2} over a 30″ beam centered on the position of the IR source. The assumption that the optical depth, τ, is small will underestimate the true column density by $\tau(1 - e^{-\tau})^{-1}$ (Plambeck, Snell, and Loren 1983). At velocities outside the self-absorption feature where C^{32}S and C^{34}S are both detected, the line ratios indicate the C^{32}S optical depth is of order unity. Since the optical depth of CS emission is expected to decrease at higher velocities in molecular outflows, our assumption that $\tau \ll 1$ is reasonable. Using the ^{13}CO column densities of Walker *et al.* (1988) measured over the same region, we derive an abundance ratio of [CS]/[^{13}CO] $= 1.6 \times 10^{-3}$. Combining this result with the [^{13}CO]/[H_2] ratio of 2.5×10^{-6} determined by Dickman (1978), we then find the [CS]/[H_2] ratio for the outflowing material to be $\approx 4 \times 10^{-9}$. This value is the same as that found by Menten *et al.* (1987) from a multitransitional LVG analysis of the CS emission observed toward the IR source at the rest velocity of the cloud. It is also similar to that found toward other warm cloud cores (Watson and Walmsley 1982). Therefore, there is no clear evidence that the CS fractional abundance in the redshifted outflowing gas has been enhanced due to shock activity.

As noted by Walker *et al.* (1988), there is no significant high-velocity blueshifted emission in their ^{13}CO spectrum. However, the strength and velocity extent of the blue and redshifted CS wing emission are about the same (see Fig. 1). This may suggest that the [CS]/[^{13}CO] abundance ratio is larger in the blueshifted gas. To further investigate this possibility, a higher signal-to-noise ^{13}CO $J = 2 \rightarrow 1$ spectrum is needed.

d) Outflow Mass and Energetics

As discussed above, the CS column density toward each position in the outflow can be estimated if we assume the emission is optically thin. The H_2 mass is then found by multiplying each column density by the area of the beam, summing the resulting product, and applying the [CS]/[H_2] ratio. Using this technique, mass estimates were made for the outflow system over the velocity intervals corresponding to those used in Figures 3 and 4.

The total mass found over the specified velocity ranges was $\sim 0.44\ M_\odot$. Since the gas was assumed to be optically thin, this mass estimate may be low by a factor of ~ 2. Also, we may have significantly underestimated the mass of the outflow, since we did not include emission at velocities where the line is heavily self-absorbed (see Fig. 1). It is reasonable to expect that a portion of the gas at these velocities participates in the outflow, since outflow related structures are seen at velocities just outside the self-absorption.

The CS derived mass is comparable to that derived for the outflow system by Walker *et al.* (1988) using ^{12}CO and ^{13}CO. Walker *et al.* also find that the outflow's mass decreases at increasing velocities. These results suggest that the bulk of the mass of molecular outflows is contained in dense, low velocity shells.

If the dense gas observed in the shell-like structures is swept-up ambient cloud material, then we can make an independent estimate of the masses of the shells. From C^{18}O measurements the ambient density throughout the region is estimated to be $\sim 2 \times 10^3$ cm^{-3} (Walker 1988). Using this value and dimensions characteristic of the outflow lobes observed in CO, the mass of swept-up material in each of the four lobes is about one solar mass. The total mass of the outflow system would then be $\sim 4\ M_\odot$. This estimate is consistent with the lower limit we derived for the outflow mass based on the CS analysis.

The momentum and energy of the high velocity gas observed in CO by Walker *et al.* (1988) is greater than that needed to

drive the shells at the observed velocities, even if the larger mass estimate derived in the previous paragraph is used. This suggests that the same engine that drives the high-velocity outflow components observed in CO is capable of driving the high-density outflow material observed in CS.

IV. SUMMARY

We mapped the region surrounding 1629a in the $C^{32}S$ $J = 2 \rightarrow 1$ transition with both the NRAO 12 m and the Hat Creek millimeter array and combined the data. Within a 2′ region surrounding the infrared source the maps are sensitive to angular resolutions from 11″ to 2′. We also took a long integration $C^{34}S$ ($J = 2$–1) spectrum toward the IR source. The principal results are:

1. Integrated intensity maps indicate that both the high-velocity and low-velocity CS emission are associated with the outflow.

2. Outside the immediate vicinity of the IR source, the CS emission appears to originate primarily from clumpy, dense ($\geq 10^4$ cm^{-3}) swept-up shells.

3. The CS fractional abundance in the outflow material is similar to that found in other warm cloud cores.

4. The bulk of the outflow system's mass is in low-velocity, shell-like structures.

5. The energy and momentum required to drive the low-velocity shells is less than that found in the high-velocity gas.

These results provide observational support for the conventional outflow model in which ambient cloud material is swept into dense, relatively low velocity shells, inside of which the higher velocity flow material propagates. We also find that the outflow(s) are a strong influence on the line formation process at all observed velocities. A large fraction of the mass of many outflow systems may be "hidden" in dense, slow moving shells.

This work was supported by NSF grant AST 87-14721 to the Radio Astronomy Laboratory, University of California, Berkeley.

REFERENCES

Bally, J., and Lada, C. J. 1983, *Ap. J.*, **265**, 824.
Cabrit, S., Goldsmith, P. F., and Snell, R. L. 1988, *Ap. J.*, **334**, 196.
Dickman, R. L. 1978, *Ap. J. Suppl.*, **37**, 407.
Fukui, Y., Sugitani, K., Takaba, H., Iwata, T., Mizuno, T., Ogawa, H., and Kawabata, K. 1986, *Ap. J. (Letters)*, **311**, L85.
Graedel, T. E., Langer, W. D., and Frerking, M. A. 1982, *Ap. J. Suppl.*, **48**, 321.
Hartquist, T. W., Oppenheimer, M., and Dalgarno, A. 1980, *Ap. J.*, **236**, 182.
Lada, C. J. 1985, *Ann. Rev. Astr. Ap.*, **23**, 267.
Menten, M., Serabyn, E., Güsten, R., and Wilson, T. 1987, *Astr. Ap.*, **182**, 127.
Plambeck, R. L., Snell, R. L., and Loren, R. B. 1983, *Ap. J.*, **266**, 321.
Snell, R. L., Loren, R. B., and Plambeck, R. L. 1980, *Ap. J. (Letters)*, **239**, L17.
Snell, R. L., Mundy, L. G., Goldsmith, P. F., Evans, N. J., and Erickson, N. R. 1984, *Ap. J.*, **276**, 625.
Takano, T. 1986, *Ap. J. (Letters)*, **300**, L85.
Thronson, H. A., and Lada, C. J. 1984, *Ap. J.*, **284**, 135.
Walker, C. K. 1988, Ph.D. thesis, University of Arizona.
Walker, C. K., Lada, C. J., Young, E. T., Maloney, P. R., and Wilking, B. A. 1986, *Ap. J. (Letters)*, **309**, L47.
Walker, C. K., Lada, C. J., Young, E. T., and Margulis, M. 1988, *Ap. J.*, **332**, 335.
Walker, C. K., Lada, C. J., Young, E. T., Margulis, M., and Wilking, B. A. 1985, *Bull. AAS*, **17**, 835.
Watson, W. D., and Walmsley, C. M. 1982, in *Regions of Recent Star Formation*, ed. R. S. Roger and P. E. Dewdney (Dordrecht: Reidel), 357.
Wilking, B. A., and Claussen, M. J. 1987, *Ap. J. (Letters)*, **320**, L133.
Wootten, A. 1989, *Ap. J.*, **337**, 858.
Wootten, A., and Loren, R. B. 1987, *Ap. J.*, **317**, 220.

JOHN H. BIEGING: 601 Campbell Hall, University of California, Berkeley, CA 94720

JOHN E. CARLSTROM: Department of Astronomy, Robinson 105-24, Caltech, Pasadena, CA 91024

CHARLES J. LADA: Steward Observatory, University of Arizona, Tucson, AZ 85721

CHRISTOPHER K. WALKER: Department of Physics, Downs Lab 320-47, Caltech, Pasadena, CA 91024

ERICK T. YOUNG: Steward Observatory, University of Arizona, Tucson, AZ 85721